Kinetic Studies on a Genetically Engineered Fused Enzyme between Rat Cytochrome P4501A1 and Yeast NADPH–P450 Reductase

Toshiyuki Sakaki,*,‡ Shiro Kominami,§ Shigeki Takemori,§ Hideo Ohkawa,∥ Megumi Akiyoshi-Shibata,‡ and Yoshiyasu Yabusaki‡

Biotechnology Laboratory, Takarazuka Research Center, Sumitomo Chemical Company, Ltd., Takarazuka, Hyogo 665, Japan, Faculty of Integrated Arts and Sciences, Hiroshima University, Higashisenda-machi, Nakaku, Hiroshima 730, Japan, and Department of Plant Protection, Kobe University, Rokkodai, Nada, Kobe 657, Japan

Received December 21, 1993; Revised Manuscript Received February 15, 1994®

ABSTRACT: Three expression plasmids, pAMC1 for rat P4501A1, pAMR2 for P4501A1 and yeast NADPH–P450 reductase, and pAFCR1 for a fused enzyme between P4501A1 and the reductase, were constructed, and each was introduced into *Saccharomyces cerevisiae* AH22 cells. The microsomal fraction prepared from the recombinant yeast cells was subjected to kinetic studies of zoxazolamine 6-hydroxylation at 10 °C. The apparent K_m and V_{max} values for hydroxylation by the fused enzyme in AH22/pAFCR1 microsomes were 0.38 mM and 0.42 s^{-1}, respectively. The rate constant for reduction of the fused enzyme with NADPH in the presence of 1 mM zoxazolamine was larger than 50 s^{-1} using a dual-wavelength stopped-flow spectrometer, indicating that electrons are rapidly transferred from NADPH through FAD and FMN to the heme iron of the fused enzyme. The rate constant k_{on} for substrate binding to the fused enzyme was 25 $mM^{-1}·s^{-1}$, which is not much different from that of nonfused P4501A1. These results together with spectral data measured during the hydroxylation reaction in the steady state suggest that the rate-limiting step of the reaction by the fused enzyme might be the release of product. On the other hand, the apparent K_m and V_{max} values for the hydroxylation of P4501A1 in AH22/pAMC1 and AH22/pAMR2 microsomes were 0.32 and 0.33 mM, and 0.015 and 0.29 s^{-1}, respectively. The rate constants for the reduction of P4501A1 were 0.025 and 0.40 s^{-1}, respectively, for AH22/pAMC1 and AH22/pAMR2 microsomes. Thus, the apparent V_{max} value and the reduction rate constant of P4501A1 in AH22/pAMR2 were about 20 times larger than those in AH22/pAMC1 in proportion to the content of NADPH–P450 reductase in the microsomal fractions. These results together with the spectral data for the hydroxylation reaction suggest that the rate-limiting step of the reaction by P4501A1 in AH22/pAMC1 and AH22/pAMR2 microsomes is the first electron transfer from NADPH–P450 reductase to P4501A1.

Cytochrome P450 monooxygenases occur widely in the biological kingdom, and more than 200 species of P450 cDNAs and genes have been cloned and characterized (Nelson et al., 1993) during the last decade. In addition, heterologous expression systems with yeast (Oeda et al., 1985; Yabusaki & Ohkawa, 1991), mammalian cells (Zuber et al., 1986), and bacteria (Larson et al., 1991) as hosts have been established. These genetic technologies have been extensively used to clarify the structure–function relationship of many P450 species.

Mammalian microsomal P450 catalyzes monooxygenase reaction in the consumption of NADPH and molecular oxygen, where electrons from NADPH are delivered with the aid of NADPH–P450 reductase. The interaction mode between P450 and NADPH–P450 reductase has been extensively studied by many investigators. Miwa et al. (1978, 1979) showed that the active molecular species in the monooxygenation reaction is a binary complex composed of P450 and NADPH–P450 reductase in rat liver microsomes and in a reconstituted system containing phospholipids. It has been shown that complex formation does not occur very rapidly in the detergent-solubilized system and also in the lipid-dispersed system (Causey et al., 1990). In the liposomal system, the rate of reduction of P450 increased linearly with increasing NADPH–P450 reductase concentration in the membrane, suggesting that the electrons were transferred from NADPH–P450 reductase to P450 through transient complex formation during the random collision of both enzymes in the membrane (Kominami et al., 1989).

The importance of the interaction between P450 and NADPH–P450 reductase has been clearly demonstrated in naturally occurring water-soluble P450BM-3 in which P450 and NADPH–P450 reductase are fused to a single protein (Fulco & Ruttinger, 1987). P450BM-3 catalyzes myristate ω2-hydroxylation at a turnover number of more than 4000 min^{-1}, which is the largest among any known reaction catalyzed by P450. Boddupalli et al. (1992) showed active complex formation between the genetically produced P450 domain and the reductase domain of P450BM-3.

Membrane-bound P450 in the fused form with the reductase, which was constructed artificially with genetic engineering, showed high monooxygenase activity as reported by Murakami et al. (1987), Yabusaki et al. (1988), Shibata et al. (1990), Sakaki et al. (1990) and Fisher et al. (1992). The optimized structure of the fused enzyme resembles the naturally occurring soluble fused enzyme P450BM-3 except for the presence of an amino-terminal membrane anchor in our fused enzymes.

In this work, we constructed three types of recombinant yeast strains. The first strain produces rat P4501A1 and yeast NADPH–P450 reductase while the expression level of the reductase is much less than P4501A1. The second strain

* Correspondence should be addressed to this author at the Biotechnology Laboratory, Takarazuka Research Center, Sumitomo Chemical Co., Ltd., 4-2-1 Takatsukasa, Takarazuka, Hyogo 665, Japan. Telephone: 81-797-74-2058. Fax: 81-797-74-2133.
‡ Sumitomo Chemical Co., Ltd.
§ Hiroshima University.
∥ Kobe University.
® Abstract published in *Advance ACS Abstracts,* April 1, 1994.

0006-2960/94/0433-4933$04.50/0

produces P4501A1 and the reductase at a ratio of 1.0:0.6. The third strain produces the fused enzyme between P4501A1 and the reductase. Using the microsomal fractions prepared from the recombinant yeast cells, kinetic studies on 6-hydroxylation of zoxazolamine, which is a skeletal muscle relaxant and a typical substrate of P4501A1 (Tomaszewski et al., 1976), were carried out. We will discuss the interaction between P4501A1 and the reductase, and the rate-limiting step of zoxazolamine 6-hydroxylation catalyzed by the fused enzyme and nonfused system.

EXPERIMENTAL PROCEDURES

Materials. DNA-modifying enzymes were purchased from Takara Shuzo Co., Ltd. (Kyoto, Japan). Zoxazolamine and NADPH were purchased from Sigma (St. Louis, MO). Sodium hydrosulfite was purchased from Wako Pure Chemicals (Osaka, Japan). ^{125}I-Protein A was purchased from Amersham Japan (Tokyo, Japan). Anti-yeast NADPH–P450 reductase Ig was kindly provided by Dr. Yuzo Yoshida of Mukogawa Women's University (Hyogo, Japan). *Escherichia coli* HB101 [F$^-$, *hsd20*, *recA3*, *ara14*, *proA2*, *LacY1*, *galK2*, *rpsL20*(*str*), *xyl-5*, *mtl-1*, *supE44*, *leuB6*, *thi-1*] (Takara Shuzo Co., Ltd.) and *Saccharomyces cerevisiae* AH22 [a, *leu2–3*, *leu2–112*, *his4–519*, *can1*) (*cir*$^+$)] were used as host strains. The modified yeast expression vector pAAH5N has been described previously (Murakami et al., 1990). The expression plasmids pAMC1 (Oeda et al., 1985) for rat P4501A1 and pAMR2 (Murakami et al., 1990) for rat P4501A1 and yeast NADPH–P450 reductase were constructed as reported previously.

Recombinant DNA Procedures. Recombinant DNA procedures and transformation of *E coli* and *S. cerevisiae* cells were performed as reported previously (Murakami et al., 1987). Linker DNAs were synthesized using an Applied Biosystems 380A DNA synthesizer. Sequencing of the synthesized linker DNA and the junction region of the constructed expression plasmid was performed following a procedure described previously (Sakaki et al., 1987).

Preparation of Microsomal Fractions of Recombinant Yeast Cells. Recombinant yeast strains were cultivated in a concentrated SD medium (Sakaki et al., 1990), and the microsomal fractions were prepared therefrom as described previously (Oeda et al., 1985). The microsomal fractions were suspended in 20 mM potassium phosphate (pH 7.4) containing 20% glycerol, 50 mM glucose, and 1 mM phenylmethanesulfonyl fluoride.

Western Blot Analysis. Microsomal fractions were subjected to electrophoresis on a 10% polyacrylamide–sodium dodecyl sulfate gel and then transferred electrophoretically from the gel to a nitrocellulose filter. The filter was probed with anti-yeast NADPH–P450 reductase Ig or anti-P4501A1 Ig, followed by ^{125}I-protein A as described previously (Oeda et al., 1985).

Zoxazolamine 6-Hydroxylation Activity. The zoxazolamine 6-hydroxylation activity of the microsomal fraction was measured in a reconstituted system containing P4501A1 or the fused enzyme (0.1–0.2 μM) in 20 mM potassium phosphate (pH 7.4), 20% glycerol, and 50 mM glucose, together with each of the following concentrations of zoxazolamine: 0.04, 0.08, 0.2, 0.4, and 0.8 mM. Glycerol was added to stabilize P4501A1 or the fused enzyme. Glucose was also added for stopped-flow analysis of NADPH–dependent heme reduction. It was noted that 20% glycerol and 50 mM glucose did not affect zoxazolamine 6-hydroxylation. The reaction was initiated by addition of NADPH to a final concentration of 200 μM. After incubation at 10 °C for 5–20 min, the reaction was stopped by vigorous mixing with 5 volumes of diethyl ether as described by Tomaszewski et al. (1976). The organic phase was recovered and analyzed on HPLC. A Waters μBondapak C18 column (3.9 mm × 300 mm) was eluted with a linear gradient of 20–50% acetonitrile aqueous solution at a flow rate of 2.0 mL/min at 30 °C. Zoxazolamine and its metabolite were detected by the absorbance at 300 nm (Tomaszewski et al., 1976). In order to estimate the coupling efficiency of NADPH utilization and hydroxylated product formation, the NADPH oxidation rate in the reaction mixture with or without 400 μM zoxazolamine was measured by following the decrease in absorbance at 340 nm based on the procedure described by Imai et al. (1977).

Preparation of 6-Hydroxyzoxazolamine. Zoxazolamine in methanol was added to the culture of the AH22/pAMR2 strain having a density of 2×10^6 cells/mL to give a final concentration of 1 mM. After further incubation at 30 °C for 24 h, the yeast cells were removed by centrifugation (3000g, 10 min), and the culture supernatant was extracted with an equal volume of diethyl ether. The resulting product was collected and analyzed by UV and mass spectra. The product was confirmed to be 6-hydroxyzoxazolamine and subsequently used as a standard sample.

Reduction Rate Measurement of Heme Iron. Stopped-flow analysis was performed at 10 °C using a dual-wavelength stopped-flow device (Unisoku Co., Ltd., Hirakata, Japan) as described previously (Kominami et al., 1992). The reaction mixture contained the microsomal fraction (0.2 μM P4501A1 or the fused enzyme), 20 mM potassium phosphate (pH 7.4), 20% glycerol, 50 mM glucose, 200 units/mL glucose oxidase, 1200 units/mL catalase, and 1 mM zoxazolamine. The reaction was initiated by rapid mixing of the microsome solution with an equal volume of 80 μM NADPH in the presence of CO, and the change in absorbance difference between 450 and 490 nm was recorded. A computer program was employed to fit the kinetic data to the equation:

$$\Delta A_{450-490}(t) = \Delta A_{450-490}(\infty)\{1 - \exp(-kt)\} \quad (1)$$

where $\Delta A(t)$ is the observed change in absorbance at time t.

Measurement of Substrate Binding. Substrate-induced difference spectra of the microsomal fraction (0.54 μM P4501A1 or the fused enzyme) were measured at zoxazolamine concentrations of 0.1, 0.2, 0.4, and 0.8 mM. Stopped-flow analysis of substrate binding was performed by mixing of the microsomes with zoxazolamine at final concentrations of 0.5 and 1.0 mM, respectively. A computer program was employed to fit the kinetic data to the equation:

$$\Delta A_{490-420}(t) = \Delta A_{490-420}(\infty)\{1 - \exp(-k_{on}[S]t)\} \quad (2)$$

where $\Delta A(t)$ is the observed change in absorbance at time t and [S] is the concentration of zoxazolamine. 6-Hydroxyzoxazolamine-induced spectra were also measured at concentrations of 0.05, 0.1, 0.2, and 0.4 mM.

Measurement of Difference Spectra during Steady-State Zoxazolamine 6-Hydroxylation. The difference spectra of the microsomal fraction were measured at 10 °C as follows. The reaction mixture of the microsomal fraction containing 0.27 μM P4501A1 or the fused enzyme, 20 mM potassium phosphate (pH 7.4), 20% glycerol, 50 mM glucose, 1 mM zoxazolamine, and 100 μM NADH was poured into both sample and reference cuvettes. NADH was used to reduce cytochrome b_5 present in the microsomes. After base-line

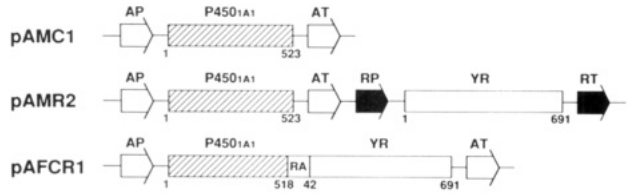

FIGURE 1: Schematic representation of the three expression plasmids: pAMC1 for rat P4501A1, pAMR2 for P4501A1 with overproduction of yeast NADPH–P450 reductase, and pAFCR1 for the fused enzyme between P4501A1 and yeast NADPH–P450 reductase. The shaded and open boxes indicate the coding regions for rat P4501A1 (P4501A1) and yeast NADPH–P450 reductase (YR), respectively. R and A indicate amino acid residues derived from the synthesized DNA linkers. The open arrows, solid arrows, and thin lines indicate the ADH promoter (AP) and terminator (AT) regions, the yeast reductase promoter (RT) and terminator (RT) regions, and the vector pAAH5N, respectively. Numbers under the coding regions indicate the number of amino acid residues as counted from the amino terminus of the corresponding enzymes.

correction, NADPH was added to the sample cuvette to a final concentration of 200 μM, and the difference spectrum from 300 to 700 nm was measured after a period of 3 min.

Other Methods. All spectral data were obtained with a Hitachi 557 spectrophotometer (Hitachi, Japan). The P450 hemoprotein concentration in whole cells and microsomal fractions was determined by a reduced CO difference spectrum as described by Omura and Sato (1964). Cytochrome *c* reductase activity was measured as described previously (Aoyama et al., 1978; Murakami et al., 1986). Cytochrome b_5 content was measured as described (Strittmatter & Velick, 1956). Protein concentration was determined by the method of Lowry et al. (1951) using bovine serum albumin as a standard. The mass spectrum of the metabolite was measured using a Hitachi DF/GC/MS M80B (Hitachi, Japan) as described previously (Sakaki et al., 1991).

RESULTS

Construction of an Expression Plasmid for a Fused Enzyme between Rat P4501A1 and Yeast NADPH–P450 Reductase. An expression plasmid, pAFCR1, for a fused enzyme between rat P4501A1 and yeast NADPH–P450 reductase was constructed following a previously described procedure (Murakami et al., 1987; Yabusaki et al., 1988a; Shibata et al., 1990; Sakaki et al., 1990). The plasmid pGYR encoding yeast NADPH–P450 reductase (Yabusaki et al., 1988b) was digested with *Pvu*II to insert a linker DNA, $^{\text{CAGCTCGAGCTG}}_{\text{GTCGAGCTCGAC}}$. The resulting plasmid was digested with *Hin*dIII and *Xho*I. The *Hin*dIII–*Xho*I fragment obtained was simultaneously inserted with a *Hin*dIII–*Xho*I fragment encoding rat P4501A1 prepared from pAMP19 (Murakami et al., 1987) into the unique *Hin*dIII site of the yeast expression vector pAAH5N to yield the expression plasmid pAFCR1. The fused enzyme thus constructed contained a linker sequence, Arg-Ala, at the junction between the P450 and reductase domains. Figure 1 schematically represents the three expression plasmids used in the present study: pAMC1 for rat P4501A1, pAMR2 for P4501A1 with overproduction of yeast NADPH–P450 reductase, and pAFCR1 for the fused enzyme between P4501A1 and the yeast reductase. Each of these expression plasmids was introduced into *S. cerevisiae* AH22 cells to obtain the corresponding recombinant yeast strains.

Expression of the Fused Enzyme in Yeast. As shown in Figure 2 (lanes A2 and B3), a protein band was detected which reacted with both anti-P4501A1 and anti-yeast reductase Ig. The migration point of the fused enzyme consists

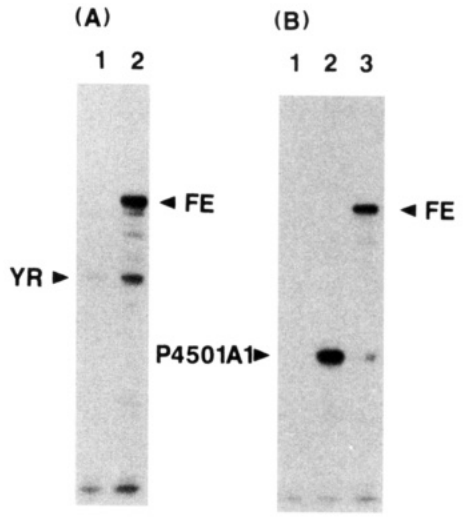

FIGURE 2: Western blot analysis of microsomal fractions prepared from recombinant yeast cells. The microsomal fraction containing 30 μg of protein was electrophoresed and then probed with anti-yeast NADPH–P450 reductase Ig (A) and anti-rat P4501A1 Ig (B). (A) Lane 1, AH22/pAAH5N (control); lane 2, AH22/pAFCR1. (B) Lane 1, AH22/pAAH5N (control); lane 2, AH22/pAMC1; lane 3, AH22/pAFCR1.

Table 1: Contents of P450, NADPH–P450 Reductase, and Cytochrome b_5 in Yeast Microsomes

strain	P450 (nmol/mg of protein)	cyt. *c* reductase act. [nmol min^{-1} (mg of protein)$^{-1}$]	cyt. b_5 (nmol/mg of protein)
AH22/pAMC1 (MC)	0.21	60	0.036
AH22/pAMR2 (MR)	0.15	860	0.039
AH22/pAFCR1 (FCR)	0.13	1720	0.055

of the molecular mass deduced from the cDNA structure. Most of the fused enzyme remained intact in the microsomal faction, while some minor bands, probably corresponding to its degradation products, were observed.

The expression level of the fused enzyme was estimated to be about 2×10^5 molecules/cell based on the CO difference spectrum of AH22/pAFCR1 cells (data not shown). The expression levels of P4501A1 in AH22/pAMC1 (Oeda et al., 1985) and AH22/pAMR2 cells (Murakami et al., 1990) were estimated to be about 4×10^5 and 3×10^5 molecules/cell, respectively.

P450, NADPH–P450 Reductase, and Cytochrome b_5 Contents in Microsomal Fractions Prepared from Recombinant Yeast Strains. P450, NADPH–P450 reductase, and cytochrome b_5 contents were determined in the microsomal fractions prepared from the recombinant yeast strains AH22/pAMC1 (MC), AH22/pAMR2 (MR), and AH22/pAFCR (FCR) (Table 1). While the P450 content in MR microsomes was slightly less than in MC microsomes, the content of NADPH–P450 reductase in MR microsomes was estimated to be 14 times larger than in the MC microsomes on the basis of cytochrome *c* reductase activity. The ratio of P4501A1 to the reductase was estimated to about 1:0.03 (mol/mol) in MC microsomes and 1:0.6 in MR microsomes on the basis of the cytochrome *c* reductase activity of the purified yeast NADPH–P450 reductase sample (Aoyama et al., 1978). For this calculation, the value 76 737 was used as the molecular weight of yeast NADPH–P450 reductase (Yabusaki et al., 1988b). This increase in the NADPH–P450 reductase content in MR microsomes is a result of overproduction of yeast NADPH–P450 reductase (Murakami, 1990). The FCR microsomes exhibited the highest cytochrome *c* reductase

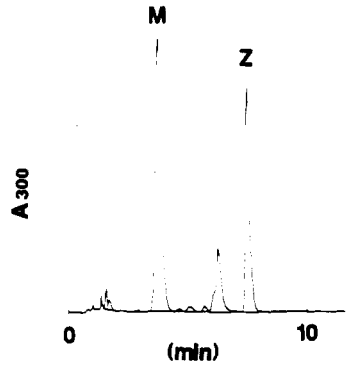

FIGURE 3: HPLC profile of zoxazolamine (Z) and its metabolite (M) in the AH22/pAMR2 cell culture supernatant. After incubation of the culture with 1 mM zoxazolamine at 30 °C for 24 h, the culture was extracted with diethyl ether and analyzed by HPLC, as described under Experimental Procedures.

Table 2: Kinetic Parameters of P4501A1 and Its Fused Enzyme for Zoxazolamine 6-Hydroxylation in Yeast Microsomes[a]

microsome	K_m (mM)	V_{max} [mol s^{-1} (mol of P450)$^{-1}$]
MC	0.32 ± 0.02	0.015 ± 0.001
MR	0.33 ± 0.02	0.29 ± 0.03
FCR	0.38 ± 0.02	0.42 ± 0.01

[a] Each value represents the mean ± SD of at least three separate experiments.

activity, suggesting that the reductase part of the fused enzyme can efficiently transfer electrons from NADPH to cytochrome *c*. The microsomal fractions of the three yeast strains contained endogenous cytochrome b_5 at a level of 0.036–0.055 nmol/mg of protein.

Zoxazolamine Metabolism by Recombinant Yeast Cells. A major zoxazolamine metabolite could be observed (Figure 3) upon addition of zoxazolamine to the culture of AH22/pAMR2 cells, whereas no metabolite of zoxazolamine was observed in the control AH22/pAAH5N cells (data not shown). The metabolite was extracted from the culture supernatant of AH22/pAMR2 as described under Experimental Procedures and subjected to EI-MS analysis (data not shown). A molecular ion (M^+) of 184 for the metabolite was noted, in contrast to a molecular ion of 168 for the substrate, indicating the metabolite to be a hydroxylated product of zoxazolamine. In addition, an absolute spectrum of the metabolite showed a peak at 300 nm (data not shown). HPLC analysis and EI-MS and UV spectra measurements conclusively showed the metabolite to be 6-hydroxyzoxazolamine (Tomaszewski et al., 1976).

Kinetics of Zoxazolamine 6-Hydroxylation Catalyzed by P4501A1 and the Fused Enzyme. In order to examine the heat stability of the microsomal fraction of the recombinant yeast cells, zoxazolamine 6-hydroxylation activity was measured after preincubation at various temperature (0–37 °C). It was found that the microsomal fractions were stable at 10 °C for at least 30 min. At higher temperatures, however, some decrease of the hydroxylation activity was observed, probably due to degradation of the yeast P450 reductase or the reductase part of the fused enzyme by endogenous proteinase in the microsomal fraction. 6-Hydroxyzoxazolamine was the only metabolite present in the reaction mixture containing P4501A1 or its fused enzyme.

Kinetic parameters for zoxazolamine 6-hydroxylation in the microsomes were estimated by Lineweaver–Burk plots and are listed in Table 2. There is not much difference in the K_m values of P4501A1 in MC and MR microsomes, and the

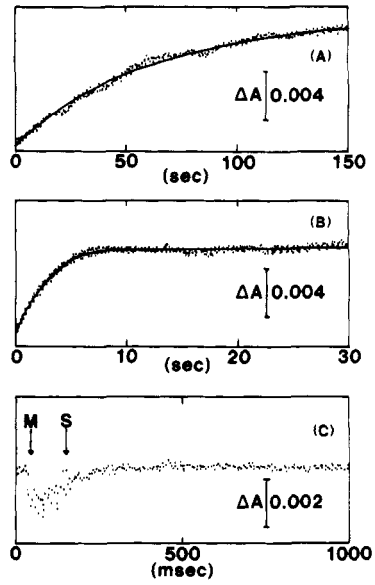

FIGURE 4: Typical kinetic traces of the reduction of P4501A1 and its fused enzyme in microsomes. The reduction of P4501A1 in AH22/pAMC1 (A), AH22/pAMR2 (B), and AH22/pAFCR1 (C) microsomes was measured at 10 °C under anaerobic conditions in the presence of CO and 1 mM zoxazolamine. The microsomal solution containing 0.2 μM P4501A1 or its fused enzyme was mixed rapidly with an equal volume of 80 μM NADPH, and the time course of increase in the absorbance difference between 450 and 490 nm was measured with a dual-wavelength device. Dotted points show data points obtained by averaging over several reactions. Solid lines in (A) and (B) show the simulated curves. In (C), M and S indicate the initiation and termination of mixing, respectively.

fused enzyme in FCR microsomes (0.32, 0.33, and 0.38 mM). The V_{max} value of P4501A1 in MR microsomes was 0.29 s^{-1}, which is 20 times larger than the V_{max} in MC microsomes (0.015 s^{-1}), approximately in proportion to the relative content of the reductase. The V_{max} value of the fused enzyme was calculated to be 0.42 s^{-1}, this being the highest among the three microsomes. Comparison of substrate-dependent NADPH utilization with the formation of 6-hydroxyzoxazolamine revealed that 85, 80, and 80% of NADPH was used for the formation of 6-hydroxyzoxazolamine in FCR, MR, and MC microsomes, respectively.

NADPH–Dependent Heme Reduction in P4501A1 and the Fused Enzyme. In the presence of the substrate zoxazolamine, about 81% of the fused enzyme was rapidly reduced. The remaining 19% was not reduced by NADPH but was reduced by sodium hydrosulfite. Nearly identical results were obtained for reduction of P4501A1 in MC and MR microsomes. Similar results on mammalian P450s have also been reported in mammalian microsomal fractions (Eyer et al., 1992).

Figure 4 shows stopped-flow analysis of the reduction of heme iron by NADPH in the presence of 1 mM zoxazolamine. The curves were optimally fitted with eq 1 described under Experimental Procedures. Although biphasic curves for heme reduction of P450 in microsomes (Peterson et al., 1976) and artificial liposomes (Taniguchi et al., 1984) have been reported, such clear biphasic behavior was not observed in this study. The rate constants *k* in MC and MR microsomes were estimated to be 0.025 and 0.40 s^{-1}, respectively (Table 3). Thus, P4501A1 in MR microsomes exhibited a 16 times larger *k* value than in the MC microsomes. Comparison of the *k* and V_{max} values for the MC and MR microsomes suggests that the first electron transfer could be the rate-limiting step of zoxazolamine 6-hydroxylation in MC and MR microsomes. On the other hand, we were not able to measure any NADPH–dependent reduction rate of the fused enzyme in FCR

Table 3: Reduction Rate Constants of P4501A1 and Its Fused Enzyme[a]

microsome	k (s^{-1})
MC	0.025 ± 0.006
MR	0.40 ± 0.05
FCR	>50

[a] Reduction of heme iron by NADPH with 1 mM zoxazolamine was measured as described under Experimental Procedures. Reduction rate constants were calculated on the basis of the equation $\Delta A_{450-490}(t) = \Delta A(\infty)\{1 - \exp(-kt)\}$. Each value represents the mean ± SD of at least four separate experiments.

Table 4: Zoxazolamine Binding Parameters of P4501A1 and Its Fused Enzyme in Yeast Microsomes[a]

microsome	K_d (mM)	k_{on} ($mM^{-1}\cdot s^{-1}$)
MC	0.27 ± 0.02	20 ± 4
MR	0.25 ± 0.02	–[b]
FCR	0.27 ± 0.01	25 ± 5

[a] Each value represents the mean ± SD value of at least three separate experiments. [b] Not tested.

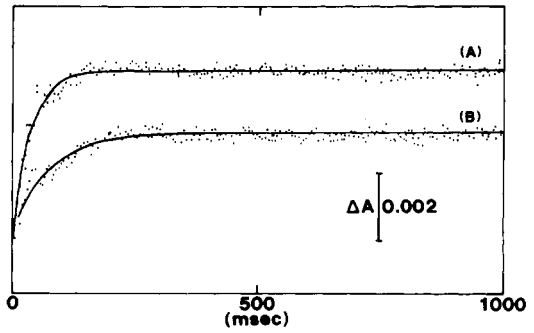

FIGURE 5: Typical kinetic traces of substrate binding to the fused enzyme in microsomes. Binding of zoxazolamine to the fused enzyme was measured at 10 °C. The microsome solution containing 0.88 μM fused enzyme was rapidly mixed with an equal volume of 2 mM (A) or 1 mM (B) zoxazolamine solution, and the increase in the absorbance difference between 490 and 420 nm was measured with a dual-wavelength stopped-flow device. Dotted points show data points obtained by averaging over several reactions, and solid lines show the simulated curves.

microsomes. The small absorbance change in Figure 4C can be explained by the assumption that most of the reaction had been completed in the dead time of the device (<20 ms).

Kinetics of Substrate Binding. The addition of zoxazolamine to the fused enzyme in FCR microsomes induced a typical type I spectrum, indicating a change of the heme iron in the fused enzyme from a low-spin state to a high-spin state upon substrate binding. Similar spectra were obtained with P4501A1 in MC and MR microsomes (data not shown). K_d values for P4501A1 in MC and MR microsomes and for the fused enzyme in FCR microsomes were estimated from double-reciprocal plots of $\Delta A_{390-420}$ and the concentration of the substrate. As shown in Table 4, both P4501A1 and its fused enzyme exhibited nearly the same affinity for the substrate. Figure 5 shows stopped-flow analysis of substrate binding of FCR microsomes. On the basis of this analysis, k_{on} values were estimated to be 20 and 25 $mM^{-1}\cdot s^{-1}$ for P4501A1 and the fused enzyme, respectively (Table 4). These data clearly indicate that substrate binding is not the rate-limiting step of zoxazolamine 6-hydroxylation in the MC, MR, and FCR microsomes even at farily lower concentration of the substrate than the K_m values.

The product 6-hydroxyzoxazolamine also induced a type I spectrum in MC, MR, and FCR microsomes. The dissociation

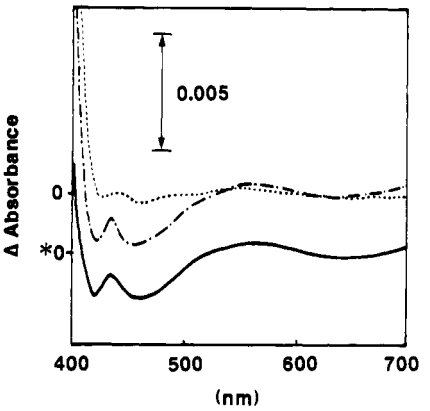

FIGURE 6: Difference spectra of microsomal fractions during steady-state zoxazolamine 6-hydroxylation. The sample and reference cuvettes contained 0.27 μM P4501A1 or the fused enzyme, 20 mM potassium phosphate (pH 7.4), 20% glycerol, 50 mM glucose, and 1 mM zoxazolamine. The reaction was started by adding 200 μM NADPH to the sample cuvette. The difference spectra were measured for AH22/pAMC1 (···), AH22/pAMR2 (– · –), and AH22/pARCR1 (—) microsomes. *0 indicates the zero point for AH22/pAFCR1.

constant of the 6-hydroxyzoxazolamine–P4501A1 complex was estimated to be 0.2 mM, which was smaller than that of the zoxazolamine–P4501A1 complex. Unfortunately, stopped-flow analysis on 6-hydroxyzoxazolamine binding could not be performed because the absorbance of 6-hydroxyzoxazolamine itself below 500 nm obscured the data.

Spectra during Steady-State Zoxazolamine 6-Hydroxylation. While the P4501A1 content in MR microsomes was nearly identical to the content in MC microsomes, their difference spectra during steady-state zoxazolamine 6-hydroxylation were quite different (Figure 6). Both spectra had a trough around 460–480 nm, but the trough in the MR microsome spectrum was much deeper than that in the MC microsome spectrum. These features were very similar to the difference spectra of the reduced versus oxidized form of NADPH–P450 reductase (Iyanagi et al., 1981; Peterson & Boddupalli, 1992). Thus, differences in the spectra between MR and MC microsomes can be clearly explained by the relative contents of NADPH-P450 reductase. In addition, the P4501A1 in MR and MC microsomes during steady-state zoxazolamine 6-hydroxylation exhibited almost the same spectrum as in the reference cuvette where most of the P4501A1 was in the ferric high-spin state.

The difference spectrum of FCR microsomes during steady-state zoxazolamine 6-hydroxylation was nearly the same as that of MR microsomes, suggesting that most of the heme iron of the fused enzyme during the steady state is in the ferric high-spin state.

DISCUSSION

We have constructed several fused enzymes, including those between rat P4501A1 and rat P450 reductase (Murakami et al., 1987; Yabusaki et al., 1988a), between bovine P450c17 and yeast P450 reductase (Shibata et al., 1990), and between bovine P450c21 and yeast P450 reductase (Sakaki et al., 1990). On the basis of these studies, the construction method derived so far for an efficient fused enzyme can be summarized as follows. First, the P450 part of the fused enzyme should be placed at the amino terminus of the fused enzyme. Second, the amino-terminal hydrophobic sequence of the reductase, a membrane anchor interacting with the lipid bilayer, should be truncated. Finally, the structure of the hinge region between P450 and reductase parts should be optimized.

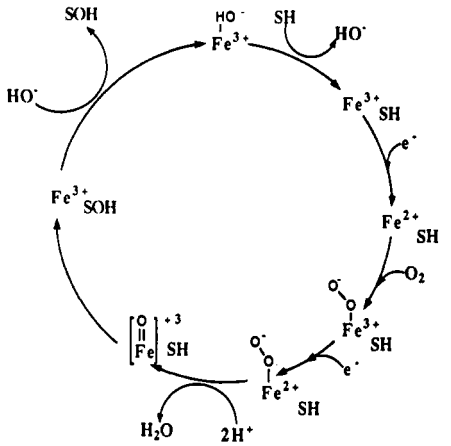

FIGURE 7: Oxidation cycle of cytochrome P450 as modified from Raag et al. (1991). SH and SOH indicate the substrate and the product, respectively.

The fused enzyme between rat P4501A1 and yeast P450 reductase in the present study was constructed according to these rules, and a high expression level of the fused enzyme in yeast could be observed. The microsomal fraction contained more than 0.1 nmol of the fused enzyme per milligram of protein, making it possible to carry out detailed kinetic studies.

We will discuss the reaction mechanism of zoxazolamine 6-hydroxylation catalyzed by the fused enzyme. The first observation in the present study is that the fused enzyme shows almost the same affinity toward the substrate as the nonfused P4501A1. This indicates that the substrate binding site in the fused enzyme is well conserved as compared with the native P4501A1. Substrate binding occurs very rapidly as indicated by stopped-flow analysis (Figure 5). In addition, a major part of the fused enzyme was not reduced by NADPH in the absence of zoxazolamine. Therefore, substrate binding seems to be the initial step of fused enzyme-dependent zoxazolamine 6-hydroxylation (Figure 7). The next step of the reaction is the first electron transfer from NADPH. The reduction rate of the heme iron of the fused enzyme is very rapid ($k > 50$ s^{-1}), and accordingly, substrate binding and the first electron transfer cannot be rate-limiting in zoxazolamine 6-hydroxylation. We did not measure directly the rate constant of the fused enzyme for O_2 binding. However, the rate constant of O_2 binding in the P450 reaction cycle is usually much larger than the rate constant for substrate binding (Peterson et al., 1972; Guengerich et al., 1976).

If the second electron transfer is rate-limiting, the fused enzyme in the steady state of the reaction must be an oxygenated form, and this would have caused a broad peak at around 430–440 nm in the difference spectrum (Imai et al., 1977). However, the spectrum (Figure 6) indicates that most of the heme iron of the fused enzyme is in a ferric high-spin state during the reaction, suggesting that the rate-limiting step is not the second electron transfer. Since almost no uncoupling occurs in NADPH utilization, no appearance of an oxygenated form in the steady state is not due to the rapid autoxidation of the oxyferro complex. The ferric high-spin form can be found in the Fe^{3+}·SOH state (Figure 7). Since the first electron transfer is not rate-limiting, most of the fused enzyme is likely to be in the Fe^{3+}·SOH state. Thus, it seems likely that the release of the product from the reaction pocket is rate-limiting in the monooxgenase reaction. Unfortunately, the k_{off} value for 6-hydroxyzoxazolamine could not be estimated because of degradation of the stopped-flow analysis due to interference by the absorbance of 6-hydroxyzoxazolamine itself.

The V_{max} value of the fused enzyme for zoxazolamine 6-hydroxylation at 37 °C was 2.9 s^{-1} (data not shown). Although this is 7 times higher than the value at 10 °C, it seems less impressive when compared with the turnover number (about 80 s^{-1}) of P450BM-3 (Narhi & Fulco, 1986). Thus, in myristate ω2-hydroxylation catalyzed by P450BM-3, all the steps comprising substrate binding, electron transfer, O–O bond cleavage, monooxygenation of the substrate, and release of the product finish within 20 ms. In the design of a more active fused enzyme for catalyzing the zoxazolamine 6-hydroxylation reaction, we should therefore consider the distal region of the heme iron of P4501A1 involved in product release.

On the other hand, the rate-limiting step of zoxazolamine 6-hydroxylation catalyzed by P4501A1 in MC microsomes is strongly suggested to be the electron-transfer process on the basis of comparison of the reductase content, the reduction rate of heme iron, and the V_{max} values of the MC and MR microsomes. If the second electron transfer is rate-limiting of the monooxygenase reaction, most of P4501A1 in MC microsomes in the steady state of the reaction must be in the oxygenated form which must cause a broad peak at around 430–440 nm in the difference spectrum. However, the spectrum shown in Figure 6 indicates no sign of the oxygenated form, suggesting that the rate-limiting step in MC microsomes is not the second but the first electron transfer. In the case of P4501A1 in MR microsomes, the first electron transfer appears to be rate-limiting judging from the heme iron reduction, although it might be possible that the first electron transfer and the product release, both of which operate on a similar time scale, are limiting.

The fused enzyme can be used as a model for a 1:1 complex of P450 and NADPH–P450 reductase which is transiently constructed on the native endoplasmic reticulum membrane. Thus, analysis of the fused enzyme can bring very important results for understanding the reaction mechanism of P450 monooxygenase. Recently, we have started flash photolysis study on the fused enzyme (Iwase et al., 1991; Ohta et al., 1994). These lines of studies will give much information about the topology and motion of each of the P450 and reductance parts of the fused enzyme on the microsomal membranes.

In conclusion, the results from the present study indicate that the fused enzyme is capable of rapidly transferring electrons from NADPH through FAD and FMN of the reductase part to the heme iron of the P450 part, as we have anticipated earlier (Murakami et al., 1987; Yabusaki et al., 1988a; Shibata et al., 1990; Sakaki et al., 1990). The rate-limiting step of the fused enzyme-catalyzed reaction is presumed to be neither the first and second electron-transfer process nor the substrate binding, but to be the release of the product. Therefore, our fused enzyme has nearly the same potentiality as P450BM-3 with regard to the efficiency of electron transfer. Recently, studies on the protein engineering of P450 by construction of chimeric P450 or site-directed mutagenesis have been reported (Imai & Nakamura, 1989; Iwasaki et al., 1993; Halper He et al., 1993; Loida & Sliger, 1993). With a combination of these new technologies, it will be possible to design highly active fused enzymes with novel activities for practical industrial processes.

ACKNOWLEDGMENT

We express our gratitude to Dr. Y. Imai of Osaka Prefecture University and Dr. Y. Yoshida of Mukogawa Women's University for stimulating discussions, and to Y. Matsuda for expert technical assistance.

REFERENCES

Aoyama, Y., Yoshida, Y., Kubota, S., Kumaoka, H., & Furumichi, A. (1978) *Arch. Biochem. Biophys. 185*, 362–369.

Boddupalli, S. S., Oster, T., Estabrook, R. W., & Peterson, J. A. (1992) *J. Biol. Chem. 267*, 10375–10380.

Causey, K. C., Eyer, C. S., & Blackes, W. L. (1990) *Mol. Pharmacol.* **38**, 134–142.

Eyer, C. S., & Backes, W. (1992) *Arch. Biochem. Biophys. 293*, 231–240.

Fisher, C. W., Shet, M. S., Caudle, D. L., Martin-Wixtrom, C. A., & Estabrook, R. W. (1992) *Proc. Natl. Acad. Sci. U.S.A. 89*, 10817–10821.

Fulco, A. J., & Ruttinger, R. T. (1987) *Life Sci. 40*, 1769–1775.

Guengerich, F. P., Ballou, D. P., & Coon, M. J. (1976) *Biochem. Biophys. Res. Commun. 70*, 951–956.

Halpert, J. R., & He, Y. (1993) *J. Biol. Chem. 268*, 4453–4457.

Imai, Y., & Nakamura, M. (1989) *Biochem. Biophys. Res. Commun. 158*, 717–722.

Imai, Y., Sato, R., & Iyanagi, T. (1977) *J. Biochem. 82*, 1237–1246.

Iwase, T., Sakaki, T., Yabusaki, Y., Ohkawa, H., Ohta, Y., & Kawato, S. (1991) *Biochemistry 30*, 8347–8351.

Iwasaki, M., Darden, T. A., Pederson, L. G., Davis, D. G., Juvonen, R. O., Sueyoshi, T., & Negishi, M. (1993) *J. Biol. Chem. 268*, 759–762.

Iyanagi, T., Makino, R., & Anan, K. (1981) *Biochemistry 20*, 1722–1730.

Kominami, S., Hara, H., Ogishima, T., & Takemori, S. (1984) *J. Biol. Chem. 259*, 2991–2999.

Kominami, S., Inoue, S., Higuchi, A., & Takemori, S. (1989) *Biochim. Biophys. Acta 985*, 293–299.

Kominami, S., Ogawa, N., Morimune, R., De-Ying, H., & Takemori, S. (1992) *J. Steroid Biochem. Mol. Biol. 42*, 57–64.

Larson, J. R., Coon, M. J., & Porter, T. D. (1991) *J. Biol. Chem. 266*, 7321–7324.

Lowry, O. H., Rosebrough, N. J., Farr, A. L., & Randall, R. J. (1951) *J. Biol. Chem. 193*, 265–275.

Murakami, H., Yabusaki, Y., & Ohkawa, H. (1986) *DNA 5*, 1–10.

Murakami, H., Yabusaki, Y., Sakaki, T., Shibata, M., & Ohkawa, H. (1987) *DNA 6*, 189–197.

Murakami, H., Yabusaki, Y., Sakaki, T., Shibata, M., & Ohkawa, H. (1990) *J. Biochem. 108*, 859–865.

Narhi, L. O., & Fulco, A. J. (1986) *J. Biol. Chem. 261*, 7160–7169.

Nelson, D. R., Kamataki, T., Waxman, D. J., Guengerich, F. P., Estabrook, R. W., Feyereisen, R., Gonzalez, F. J., Coon, M. J., Gunsalus, I. C., Gotoh, O., Okuda, K., & Nebert, D. W. (1993) *DNA Cell Biol. 12*, 1–51.

Oeda, K., Sakaki, T., & Ohkawa, H. (1985) *DNA 4*, 203–210.

Ohta, Y., Sakaki, T., Yabusaki, Y., Ohkawa, H., & Kawato, S. (1994) *J. Biol. Chem.* (in press).

Omura, T., & Sato, R. (1964) *J. Biol. Chem. 239*, 2370–2378.

Peterson, J. A., & Bodddupalli (1992) *Arch. Biochem. Biophys. 294*, 654–661.

Peterson, J. A., Ishimura, Y., & Griffin, B. W. (1972) *Arch. Biochem. Biophys. 149*, 197–208.

Peterson, J. A., Ebel, R. E., O'Keeffe, D. H., Matsubara, T., & Estabrook, R. W. (1976) *J. Biol. Chem. 251*, 4010–4016.

Raag, R., Martinis, S. A., Sliger, S. G., & Poulos, T. L. (1991) *Biochemistry 30*, 11420–11429.

Ruettinger, R. T., Wen, L. P., & Fulco, A. J. (1989) *J. Biol. Chem. 264*, 10987–10995.

Sakaki, T., Shibata, M., Yabusaki, Y., Murakami, H., & Ohkawa, H. (1987) *DNA 6*, 31–39.

Sakaki, T., Shibata, M., Yabusaki, Y., Murakami, H., & Ohkawa, H. (1990) *DNA Cell Biol. 9*, 603–614.

Sakaki, T., Akiyoshi-Shibata, M., Yabusaki, Y., Manabe, K., Murakami, H., & Ohkawa, H. (1991) *Pharmacogenetics 1*, 86–93.

Shibata, M., Sakaki, T., Yabusaki, Y., Murakami, H., & Ohkawa, H. (1990) *DNA Cell Biol. 9*, 27–36.

Strittmater, P., & Velick, S. F. (1956) *J. Biol. Chem. 221*, 253–264.

Taniguchi, H., Imai, Y., & Sato, P. (1984) *Arch. Biochem. Biophys. 232*, 585–596.

Tomaszewski, J. E., Jerina, D. M., Levin, W., & Conney, A. H. (1976) *Arch. Biochem. Biophys. 176*, 788–798.

Yabusaki, Y., & Ohkawa, H. (1991) in *Frontiers in Biotransformation* (Ruckpaul, K., & Rein, H., Eds.) Vol. 4, pp 169–190, Akademie Verlag, Berlin.

Yabusaki, Y., Murakami, H., Sakaki, T., Shibata, M., & Ohkawa, H. (1988a) *DNA 7*, 701–711.

Yabusaki, Y., Murakami, H., & Ohkawa, H. (1988b) *J. Biochem. 103*, 1004–1010.

Zuber, M. X., John, M. E., Okamura, T., Simpson, E. R., & Waterman, M. R. (1986) *J. Biol. Chem. 261*, 2475–2482.